reduced LVEF (HFrEF) or hypertension have not shown consistent benefits for HFpEF.[16] At present, the treatment for acute decompensated heart failure is largely empirical, focusing on blood pressure control and treatment or avoidance of intravascular volume overload.[7] There is a need to focus on the precise mechanisms of volume intolerance in acute decompensated heart failure.

The stressed blood volume and systemic blood pressure are controlled by several systems. Among them, the arterial baroreflex system is an important and powerful regulator.[17–19] Arterial baroreceptors are stretch receptors located within the arterial wall of elastic vessels such as the aortic arch and carotid sinuses. The arterial baroreflex is impaired in patients with both HFrEF and HFpEF.[20] LV diastolic dysfunction is induced by arterial baroreflex failure (FAIL).[21] Many studies have revealed that major risk factors of HFpEF, such as aging, hypertension, diabetes, renal insufficiency, and atherosclerosis, are closely associated with FAIL.[5,22–26]

Therefore, we hypothesized that FAIL plays a pivotal role in the pathogenesis of volume intolerance in acute decompensated heart failure regardless of LVEF. To test this hypothesis, we developed a FAIL model in rats with normal LV function and assessed the LAP and systemic arterial pressure (AP) responses to volume overload. Furthermore, to study the reversibility of impaired volume tolerance in the FAIL model, we tested a novel artificial (bionic) arterial baroreflex system that we reported recently.[27]

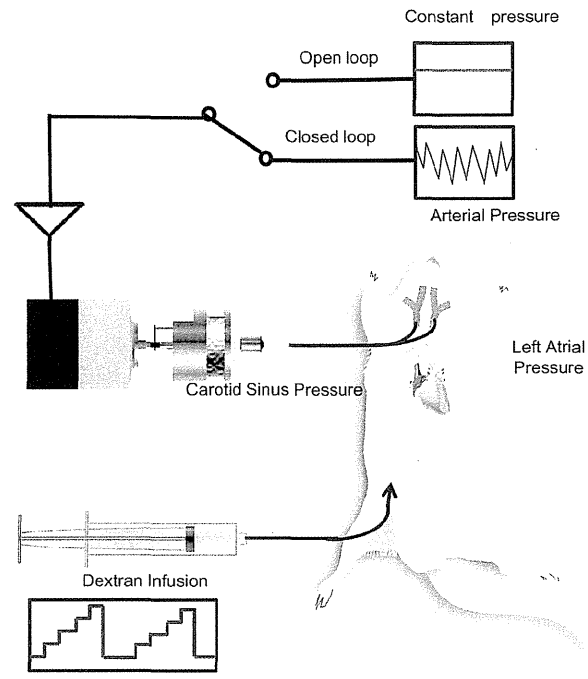

Fig. 1. Schematic representation of the preparation in the present study. Responses in arterial pressure and left atrial pressure after stepwise volume infusion were compared under native open-loop arterial baroreflex conditions (switching upward) and closed-loop arterial baroreflex conditions (switching downward).

Methods

Animals

All procedures and animal care were approved by the Committee on Ethics of Animal Experiment, Kyushu University Graduate School of Medical and Pharmaceutical Sciences, and were performed in accordance with the Guideline for Animal Experiment of Kyushu University. Five 14- to 16-week-old male Sprague-Dawley rats (SLC, Hamamatsu, Japan) weighing 450–650 g were used.

Surgical Preparations

Figure 1 illustrates the experimental preparation. Rats were anesthetized by intraperitoneal injection (2 mL/kg) of a mixture of urethane (250 mg/mL) and α-chloralose (40 mg/mL). Anesthesia was maintained by continuous intravenous infusion of the anesthetics at a rate of 0.1 mL/kg/h with the use of a syringe pump (CFV-3200; Nihon Kohden, Tokyo, Japan). Lactated Ringer solution also was infused continuously (6 mL/kg/h) to prevent dehydration. The rats were intubated and ventilated artificially with room air (SN-480-7; Shinano, Tokyo, Japan). We vascularly isolated bilateral carotid sinuses from the systemic circulation as reported previously.[17–19] Carotid sinuses were isolated and filled with lactated Ringer solution through catheters inserted via the common carotid arteries. We measured the carotid sinus pressure (CSP) with the use of a fluid-filled pressure transducer (AP-630G; Nihon Kohden) and controlled CSP with the use of a servo-controlled piston pump (ET-126A; Labworks, Costa Mesa, California). Bilateral vagal nerves were sectioned at the middle of the neck to eliminate reflexes from the cardiopulmonary region and to prevent efferent conduction. Bilateral aortic depressor nerves were sectioned to eliminate the reflexes from the aortic arch. Using this preparation, we mimicked the normal arterial baroreflex (NORM) by matching CSP to instantaneous AP (closed loop) and FAIL by maintaining CSP at a constant value regardless of AP perturbations (open loop).

Protocols

We infused dextran stepwise every minute in a volume of 1–4 mL/kg until LAP reached 14–16 mm Hg and measured LAP and AP in response to the infused volume (Vi). The measurements were repeated in alternating interleaved fashion in NORM and FAIL. Each volume challenge was followed by blood withdrawal until CSP, LAP, and systemic AP returned to the basal level. The sequence of the volume challenge was randomized to minimize order bias.

Bionic Arterial Baroreflex System

To implement arterial baroreflex transduction as a native arterial baroreceptor (bionic arterial baroreflex system), we stimulated afferent nerves (the aortic depressor nerve) in a previously reported fashion.[27] In brief, the bionic arterial baroreflex system consists of an arterial pressure sensor (DX-360, MEG-5200; Nihon Kohden), a neurostimulator (SEN-3401, Nihon Kohden; AD202JN, Analog Devices, Norwood, Massachusetts), and a regulator (Studio 1410; Dell, Round Rock, Texas). The bionic pressure sensor senses AP, and the regulator translates AP into neurostimulation (stimulation of the aortic depressor nerve), thus mimicking the native arterial baroreceptor. Therefore, the bionic baroreflex system is expected to substitute impaired baroreceptors.

The neurostimulator generates an electrical rectangular pulse train (5 V intensity, 0.2 ms pulse width) according to the command signal from the regulator. The regulator updates the frequency of the pulse train every 10 ms. The encoding rule for translating intracarotid sinus pressure into stimulation of the aortic depressor nerve was identified with the use of a white noise technique and applied to the regulator.

Data Acquisition and Analysis

We recorded the pressures and digitalized the recordings at a sampling rate of 200 Hz with the use of a 12-bit analog-to-digital converter. The 10-s data of LAP and AP starting from 50 s after dextran infusion were used in the analysis.

Statistical Analysis

The data are presented as least-squares mean ± standard error. Multiple data sets of NORM (repeated twice) and FAIL (repeated twice) were compared using a linear mixed-effects model. Rat identity was specified as a random effect. Assumptions of normality and homoscedasticity were fulfilled. The linear mixed-effects models were carried out using JMP version 9.0.2 (SAS Institute, Cary, CA, USA). The estimated values from the mixed-effect model are presented as least squares mean ± standard error. Differences were considered to be significant when the P value was $<.05$. Curve fitting in nonlinear regression was performed with the use of Graphpad Prism version 5.04 (Graphpad, San Diego, California).

Results

Baseline Characteristics

The heart rate, mean AP (mAP), and LAP before volume load sequences are presented in Table 1. Baseline hemodynamic parameters did not differ significantly between NORM and FAIL.

Representative Recording

Figure 2 shows representative recordings of AP, CSP, and LAP in response to stepwise dextran infusion. In NORM, matching AP and CSP indicated normal activation of the arterial baroreflex. In contrast, in FAIL, CSP was unaltered despite AP perturbation, indicating no arterial baroreflex activation. In NORM, volume loading by dextran infusion reproducibly increased both LAP and AP, but the changes were relatively small. In FAIL, however, a much smaller volume load increased LAP and AP markedly, indicating striking volume intolerance. Before switching from FAIL to NORM or NORM to FAIL, we terminated volume infusion and determined the recovery of CSP, AP, and LAP to each basal level. Duration of the entire experiment from anesthesia induction to killing the animal under artificial ventilation was ~4 hours.

Table 1. Baseline Hemodynamic Parameters

	NORM	FAIL	P
HR (bpm)	433.4 ± 10.8	433.7 ± 10.9	NS
mAP (mm Hg)	90.5 ± 5.4	85.2 ± 5.3	NS
LAP (mm Hg)	6.6 ± 0.5	6.4 ± 0.5	NS

bpm, beats per minute; FAIL, arterial baroreflex failure; HR, heart rate; LAP, left atrial pressure; mAP, mean arterial pressure; NORM, normal arterial baroreflex; NS, not significant. Values are least-squares means ± standard error.

LAP-Vi Relationship

The volume load intolerance in FAIL is clearly demonstrated in the plot of the LAP-Vi relationship (Fig. 3A). The LAP-Vi relationship was markedly steeper in FAIL than in NORM, indicating that FAIL induces significant volume intolerance.

To quantify the LAP sensitivity to volume load, we fitted a monoexponential curve [LAP = Exp (AVi) + B, where A denotes the coefficient of the curve and B is a constant] to the LAP-Vi relationship (Fig. 3B). The coefficient of the monoexponential curve (A), an index of LAP sensitivity to Vi, was significantly higher in FAIL than in NORM (0.27 ± 0.03 vs 0.16 ± 0.03; n = 10; $P < .01$).

Critical Volume to Provoke Pulmonary Edema

To assess the extent of volume load intolerance that provokes pulmonary edema, we estimated critical Vi as the Vi at which LAP reaches 20 mm Hg.[28] As shown in Figure 4, critical Vi was significantly smaller in FAIL than in NORM (15.0 ± 1.6 mL/kg vs 19.4 ± 1.6 mL/kg; n = 10; $P < .01$), indicating that FAIL induces volume load intolerance The least-squares mean of differences between NORM and FAIL was 4.5 ± 1.2 mL/kg, which represents one-fifth of the stressed volume.

LAP in response to the same volume load was compared between NORM and FAIL. At the critical Vi for FAIL (19.4 mL/kg), LAP was by definition 20 mm Hg in FAIL but was significantly and markedly lower in NORM (8.6 ± 2.3 mm Hg; $P < .01$).

AP-Vi Relationship

Figure 5A shows the mAP-Vi relationship. For a given Vi, mAP was consistently higher in FAIL than in NORM. We fitted a logarithmic curve [mAP = A × ln (Vi − B), where A denotes the coefficient of the curve and B is a constant] to the mAP-Vi relationship . The coefficient of the logarithmic curve (A) was significantly higher in FAIL than in NORM (69.0 ± 3.3 vs 49.1 ± 3.3; n = 10; $P < .01$), indicating that AP is supersensitive to volume overload under FAIL conditions.

We examined the systolic AP at which LAP reached 20 mm Hg (ie, at the critical Vi). Systolic AP at the critical Vi was significantly higher in FAIL than in NORM (194 ± 6 mm Hg vs 163 ± 6 mm Hg; n = 10; $P < .01$; Fig. 5B). The least-squares mean of differences in systolic AP between NORM and FAIL was 30 ± 6 mm Hg.

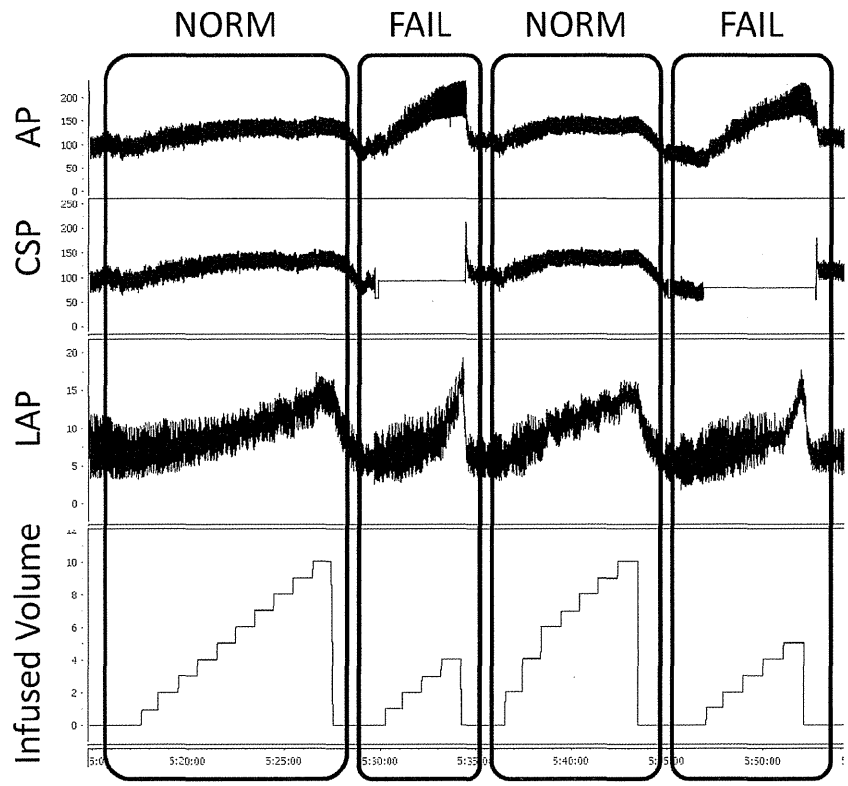

Fig. 2. Typical example of recordings obtained during volume loading by dextran infusion. Arterial blood pressure (AP), carotid sinus pressure (CSP), left atrial pressure (LAP), and volume of dextran infused (Infused Volume) are shown. FAIL, arterial baroreflex failure; NORM, normal arterial baroreflex.

Benefit of Bionic Arterial Baroreflex System on Volume Intolerance

Typical recordings are shown in Figure 6A. Our bionic arterial baroreflex system was able to fully reverse the physiologic volume intolerance in the FAIL animals (Fig. 6B).

Discussion

We demonstrated that the estimated critical volume load at which LAP reaches 20 mm Hg was significantly smaller and systemic AP at the critical volume load was significantly higher under FAIL conditions mimicked by constant CSP than under NORM conditions. These findings indicate that FAIL induces volume intolerance with an increase in systemic AP with normal LV function. FAIL might be involved in the pathogenesis of acute decompensated heart failure with a striking increase in LAP regardless of LVEF.

The novel finding is that volume intolerance was prominent in FAIL with normal LV function. Because all animals in the present study had normal LV function, we can consider that LV dysfunction was not a prerequisite for

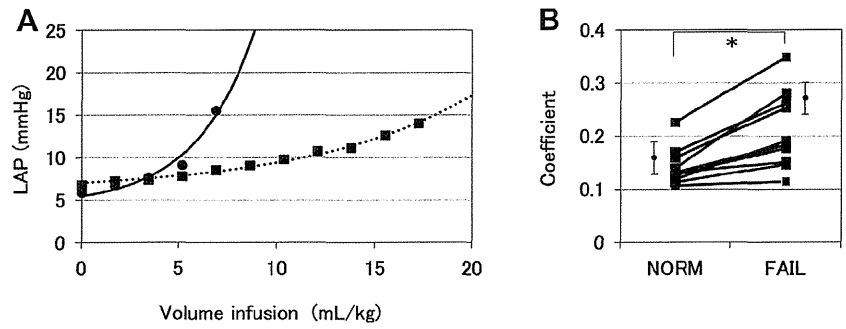

Fig. 3. (A) Typical example of the response of left atrial pressure (LAP) to infused volume (Vi) of dextran. We fitted a monoexponential curve [LAP = Exp (AVi) + B] to the LAP-Vi relationship. The curves were drawn from the least-squares means of the fitting parameters under normal arterial baroreflex (NORM; dotted line) and arterial baroreflex failure (FAIL; solid line) conditions. (B) Summarized data of the LAP-Vi relationship. Coefficient of the monoexponential curve was significantly higher in FAIL than in NORM (0.27 ± 0.03 vs 0.16 ± 0.03; n = 10; $P < .01$). *Significantly different means (Tukey post hoc comparison).

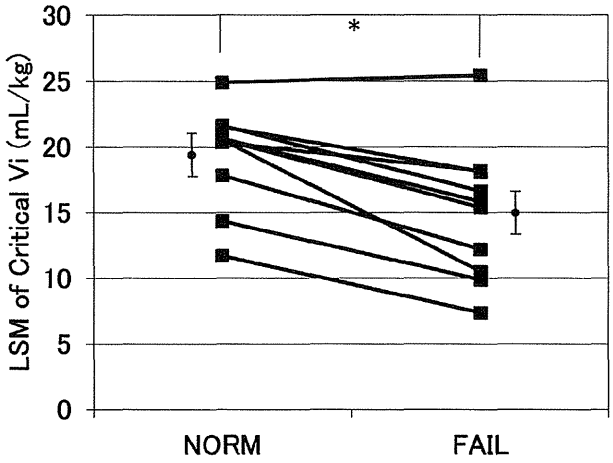

Fig. 4. Effect of baroreflex failure on critical infused volume (Vi) at which left atrial pressure reaches 20 mm Hg. The points of the least-squares means (LSMs) of each subject are connected. *Significantly different means (Tukey post hoc comparison; $P < .05$). The number of repeated measures was 10 for both normal arterial baroreflex (NORM) and arterial baroreflex failure (FAIL).

volume intolerance. This model could explain the unique feature of acute decompensated heart failure. Although the pathophysiology of HFpEF was initially thought to be due principally to LV diastolic dysfunction, recent studies have suggested more complex involvement of multiple abnormalities.[29,30] Risk factors are closely similar between in HFpEF and FAIL.[5,7,25,26] Considering these earlier findings, our present results may suggest that FAIL could be one of the cardinal causes of volume intolerance in acute decompensated heart failure regardless of LV function.

The cardiopulmonary baroreflex is also quite important in the pathogenesis of heart failure via autonomic regulation.[20] However, our present results indicate the effect of the arterial baroreflex on volume tolerance, because we did vagal sectioning that would lead to the exclusion of the cardiopulmonary baroreflex. Moreover, the effect of the arterial baroreflex on volume tolerance should be quite important clinically, because sympathetic nerve activity and gain of the arterial baroreflex is significantly smaller in the anesthetized condition than in the conscious state.[31] In addition, our results could support the concept that redistribution rather than net accumulation of fluid might contribute importantly to acute decompensated heart failure.

Risk factors of HFpEF are quite similar to those of FAIL.[5,25,26] Atherosclerosis stiffens the arterial wall in which the arterial baroreflex receptors are located.[22–24] Chronic hypertension and cardiovascular changes associated with aging are the most common causes of HFpEF.[7] Pulse wave velocity is increased in HFpEF to a greater extent than in HFrEF.[32] These clinical findings also support the notion that FAIL is one of the main factors in HFpEF pathogenesis regardless of LV dysfunction. However, it has not been clarified whether FAIL induces the transient and repeated increase in LAP in acute decompensated heart failure. The present study provides a novel concept that FAIL induces, in part, striking volume intolerance in the absence of LV dysfunction. Furthermore, to prevent flash pulmonary edema in acute decompensated heart failure, we should focus on not only LV dysfunction but also FAIL, in addition to attenuation of atherosclerotic risk factors.

Approximately one-half of the patients with heart failure have HFpEF, and the morbidity and mortality are similar to HFrEF. Therapies with unequivocal benefit for HFrEF, such as angiotensin-converting enzyme inhibitors, β-blockers, diuretics, and digitalis, have not shown consistent benefits for HFpEF.[16] Because the major risk factors of HFpEF are known to promote atherosclerosis,[5,25,26] statins given for the treatment of atherosclerosis could be effective for HFpEF. In support of this observation, a clinical study with a mean follow-up of 21 months indicated that statin therapy was associated with significantly lower mortality in patients with diastolic heart failure.[33] However, the GISSI-HF trial that evaluated the effectiveness of rosuvastatin on death or cardiovascular hospitalization in patients with chronic heart failure found no benefit in the subgroup of patients with HFpEF.[34] Direct carotid sinus stimulation has been proposed as a nonpharmacologic therapy, because this therapy might improve symptoms in patients with heart failure through reducing heart rate, improving baroreflex

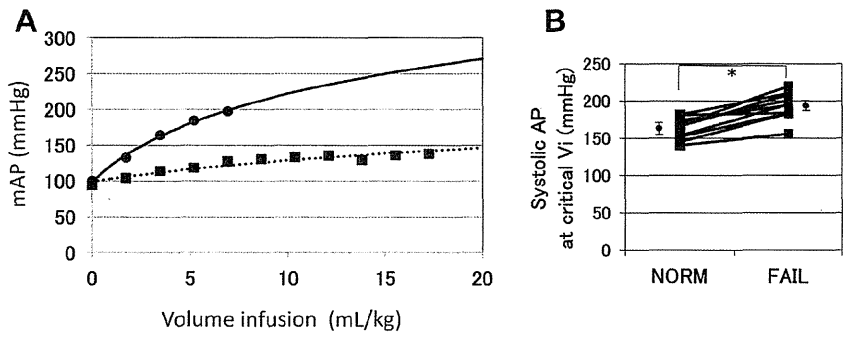

Fig. 5. (A) Response of mean arterial pressure (mAP) to infused volume (Vi) of dextran. We fitted a logarithmic curve [mAP = A × ln (Vi − B)] to the mAP-Vi relationship. The curves were drawn from the least-squares means of the fitting parameters under normal arterial baroreflex (NORM; dotted line) and arterial baroreflex failure (FAIL; solid line) conditions. (B) Systolic arterial pressure (AP) at critical Vi for FAIL under NORM and FAIL conditions. *Significantly different means (Turkey post hoc comparison).

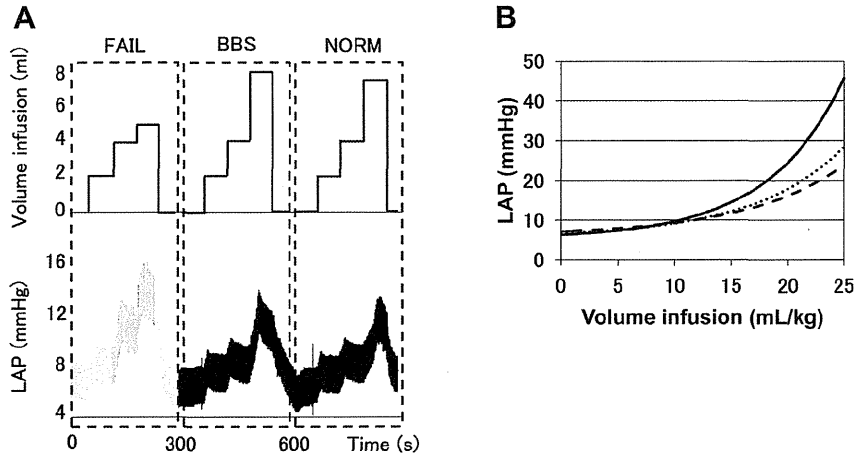

Fig. 6. (A) Typical recordings of changes in left atrial pressure (LAP) in response to infused volume (Vi) of dextran under arterial baroreflex failure (FAIL), bionic arterial baroreflex system (BBS), and normal arterial baroreflex (NORM) conditions. (B) Summarized data of LAP-Vi relationship in FAIL (solid line), BBS (dashed line), and NORM (dotted line).

sensitivity, altering nitric oxide bioavailability, antiarrhythmic effects, or central modulation.[35] However, the effects of parasympathetic activation on HFpEF have not been fully clarified. Given these results, we should recognize that the proven therapies for HFpEF are not consistent and that the treatment for acute decompensating heart failure is largely empirical, focusing on blood pressure control and treatment or avoidance of intravascular volume overload.[16,36] The present study provides a possible concept for the precise mechanisms of flash pulmonary edema in acute decompensated heart failure, in both HFpEF and HFrEF.

Interestingly, our bionic arterial baroreflex system was able to fully reverse the physiologic volume intolerance in FAIL. These results could suggest that the bionic arterial baroreflex system would be an attractive therapeutic tool in preventing volume intolerance in acute decompensated heart failure. A recent study also indicated that arterial baroreflex activation could be a novel therapeutic strategy for diastolic heart failure.[37] To develop a clinically useful system, further investigations to develop durable pressure sensors and electrodes are essential.

Study Limitations

There are several limitations to the present study. First, our model creates a condition of absolute FAIL mimicked by constant CSP, and the arterial baroreceptor of the carotid sinus is unable to perceive any change in blood pressure. In the clinical situation, patients with atherosclerosis of the carotid sinus may have impaired arterial baroreflex transduction, but they maintain at least marginal baroreflex function. Therefore, the difference in the clinical situation could be smaller than our estimation. On the other hand, because the surgical procedure and injury to the carotid sinus may damage NORM function, the difference in patients could be larger than our estimation. However, the importance of this study is that the arterial baroreflex system is capable of preventing striking volume intolerance regardless of LVEF. Second, we defined the critical volume as the infused volume resulting in LAP at 20 mm Hg. However, we continued the volume infusion until LAP was 14–16 mm Hg, and the critical volume was only estimated because it was necessary for us to repeat NORM and FAIL in the same rat. Volume infusion resulting in LAP at 20 mm Hg caused the real flash pulmonary edema, and we were not able to continue the experiments. Third, we fitted only a monoexponential curve to the obtained data of LAP and Vi, and we could not exclude a third curve that is not quite vertical (Fig. 3A). However, even if there is a third curve, we also consider that the LAP-Vi relationship was still markedly steeper in FAIL than in NORM, and we can conclude that FAIL induces significant volume intolerance.

Conclusion

FAIL induces, in part, striking volume intolerance with an increase in systemic AP in a rat model with normal LV function. Extrapolating this finding to patients with acute decompensated heart failure, FAIL might greatly increase the sensitivity to volume overload irrespective of LV function.

Disclosures

None.

References

1. Gandhi SK, Powers JC, Nomeir AM, Fowle K, Kitzman DW, Rankin KM, Little WC. The pathogenesis of acute pulmonary edema associated with hypertension. N Engl J Med 2001;344:17–22.
2. Konishi M, Maejima Y, Inagaki H, Haraguchi G, Hachiya H, Suzuki J, et al. Clinical characteristics of acute decompensated heart failure with rapid onset of symptoms. J Card Fail 2009;15:300–4.

3. Gheorghiade M, Abraham WT, Albert NM, Greenberg BH, O'Connor CM, She L, et al. Systolic blood pressure at admission, clinical characteristics, and outcomes in patients hospitalized with acute heart failure. JAMA 2006;296:2217–26.
4. Bier AJ, Eichacker PQ, Sinoway LI, Terribile SM, Strom JA, Keefe DL. Acute cardiogenic pulmonary edema: clinical and noninvasive evaluation. Angiology 1988;39:211–8.
5. Banerjee P, Clark AL, Nikitin N, Cleland JGF. Diastolic heart failure. Paroxysmal or chronic? Eur J Heart Fail 2004;6:427–31.
6. Vasan RS, Benjamin EJ, Levy D. Prevalence, clinical features and prognosis of diastolic heart failure: an epidemiologic perspective. J Am Coll Cardiol 1995;26:1565–74.
7. Massie BM, Carson PE, McMurray JJ, Komajda M, McKelvie R, Zile MR, et al. Irbesartan in patients with heart failure and preserved ejection fraction. N Engl J Med 2008;359:2456–67.
8. Aurigemma GP, Gaasch WH. Clinical practice: diastolic heart failure. N Engl J Med 2004;351:1097–105.
9. Aurigemma GP, Zile MR, Gaasch WH. Contractile behavior of the left ventricle in diastolic heart failure: with emphasis on regional systolic function. Circulation 2006;113:296–304.
10. Kitzman DW, Little WC, Brubaker PH, Anderson RT, Hundley WG, Marburger CT, et al. Pathophysiological characterization of isolated diastolic heart failure in comparison to systolic heart failure. JAMA 2002;288:2144–50.
11. Baicu CF, Zile MR, Aurigemma GP, Gaasch WH. Left ventricular systolic performance, function, and contractility in patients with diastolic heart failure. Circulation 2005;111:2306–12.
12. Lam CSP, Roger VL, Rodeheffer RJ, Bursi F, Borlaug BA, Ommen SR, et al. Cardiac structure and ventricular-vascular function in persons with heart failure and preserved ejection fraction from Olmsted County, Minnesota. Circulation 2007;115:1982–90.
13. Melenovsky V, Borlaug BA, Rosen B, Hay I, Ferruci L, Morell CH, et al. Cardiovascular features of heart failure with preserved ejection fraction versus nonfailing hypertensive left ventricular hypertrophy in the urban Baltimore community. J Am Coll Cardiol 2007;49:198–207.
14. Ahmed SH, Clark LL, Pennington WR, Webb CS, Bonnema DD, Leonardi AH, et al. Matrix metalloproteinases/tissue inhibitors of metalloproteinases: relationship between changes in proteolytic determinants of matrix composition and structural, functional and clinical manifestations of hypertensive heart disease. Circulation 2006;113:2089–96.
15. Zile MR, Baicu CF, Gaasch WH. Diastolic heart failure: abnormalities in active relaxation and passive stiffness of the left ventricle. N Engl J Med 2004;350:1953–9.
16. Owan TE, Hodge DO, Herges RM, Jacobsen SJ, Roger VL, Redfield MM. Trends in prevalence and outcome of heart failure with preserved ejection fraction. N Engl J Med 2006;355:251–9.
17. Shoukas AA, Callahan CA, Lash JM, Haase EB. New technique to completely isolate carotid sinus baroreceptor regions in rats. Am J Physiol 1991;260:H300–3.
18. Sato T, Kawada T, Inagaki M, Shishido T, Takaki H, Sugimachi M, Sunagawa K. New analytic framework for understanding sympathetic baroreflex control of arterial pressure. Am J Physiol 1999;276:H2251–61.
19. Sato T, Kawada T, Miyano H, Shishido T, Inagaki M, Yoshimura R, et al. New simple methods for isolating baroreceptor regions of carotid sinus and aortic depressor nerves in rats. Am J Physiol 1999;276:H326–32.
20. Floras JS. Sympathetic nervous system activation in human heart failure: clinical implications of an updated model. J Am Coll Cardiol 2009;54:375–85.
21. Mostarda C, Moraes-Silva IC, Moreira ED, Medeiros A, Piratello AC, Comsolim-Colombo FM, et al. Baroreflex sensitivity impairment is associated with cardiac diastolic dysfunction in rats. J Cardiac Fail 2011;17:519–25.
22. Kaushal P, Taylor JA. Inter-relations among declines in arterial distensibility, baroreflex function and respiratory sinus arrhythmia. J Am Coll Cardiol 2002;39:1524–30.
23. Protogerou AD, Stergiou GS, Lourida P, Achimastos A. Arterial stiffness and orthostatic blood pressure changes in untreated and treated hypertensive subjects. J Am Soc Hypertens 2008;2:372–7.
24. Ueno LM, Miyachi M, Matsui T, Takahashi K, Yamazaki K, Hayashi K, et al. Effect of aging on carotid artery stiffness and baroreflex sensitivity during head-out water immersion in man. Braz J Med Biol Res 2005;38:629–37.
25. Kliger C, King DL, Maurer MS. A clinical algorithm to differentiate heart failure with a normal ejection fraction by pathophysiologic mechanism. Am J Geriat Cardiol 2006;15:50–7.
26. Gaasch WH, Zile MR. Left ventricular diastolic dysfunction and diastolic heart failure. Annu Rev Med 2004;55:373–94.
27. Hosokawa K, Ide T, Tobushi T, Sakamoto K, Onitsuka K, Sakamoto T, et al. Bionic baroreceptor corrects postural hypotension in rats with impaired baroreceptor. Circulation 2012;126:1278–85.
28. Saldias FJ, Azzam ZS, Ridge KM, Yeldandi A, Rutschman DH, Schraufnagel D, Sznajder JI. Alveolar fluid reabsorption is impaired by increases left arterial pressures in rats. Am J Physiol 2001;281:L591–7.
29. Ho JE, Gona P, Pencina MJ, Tu JV, Austin PC, Vasan RS, et al. Discriminating clinical features of heart failure with preserved vs reduced ejection fraction in the community. Eur Heart J 2012;33:1734–41.
30. Burkhoff D, Maurer MS, Packer M. Heart failure with a normal ejection fraction: is it really a disorder of diastolic function? Circulation 2003;107:656–8.
31. Thrasher TN. Unloading arterial baroreceptors causes neurogenic hypertension. Am J Physiol 2002;282:R1044–53.
32. Balmain S, Padmanabhan N, Ferrell WR, Morton JJ, McMurray JJ. Differences in arterial compliance, microvascular function and venous capacitance between patients with heart failure and either preserved or reduced left ventricular systolic function. Eur J Heart Fail 2007;9:865–71.
33. Fukuta H, Sane DC, Brucks S, Little WC. Statin therapy may be associated with lower mortality in patients with diastolic heart failure: a preliminary report. Circulation 2005;112:357–63.
34. Tavazzi L, Maggioni AP, Marchioli R, Barlera S, Franzosi MG, Latini R, et al. Effect of rosuvastatin in patients with chronic heart failure (the GISSI-HF trial): a randomized, double-blind, placebo-controlled trial. Lancet 2008;372:1231–9.
35. Borlaug BA, Melenovsky V, Russell SD, Kessler K, Pacak K, Becker LC, Kass DA. Impaired chronotropic and vasodilator reserves limit exercise capacity in patients with heart failure and a preserved ejection fraction. Circulation 2006;114:2138–47.
36. Hunt SA, Abraham WT, Chin MH, Feldman AM, Francis GS, Ganiats TG, et al. 2009 Focused update incorporated into the ACC/AHA 2005 guidelines for the diagnosis and management of heart failure in adults: a report of the American College of Cardiology Foundation/American Heart Association Task Force on Practice Guidelines: developed in collaboration with the International Society for Heart and Lung Transplantation. Circulation 2009;119:e391–479.
37. Brandt MC, Madershahian N, Velden R, Hoppe UC. Baroreflex activation as a novel therapeutic strategy for diastolic heart failure. Clin Res Cardiol 2011;100:249–51.

Multidisciplinary Approach to Genome-Wide Association Study for Heart Failure Based on the Different Ethnicity

-An overview of the bioinformatics and a new concept of BWAS-

Teruhiko Toyo-oka[1)]*, Licht Toyo-oka[2)]*, Manfred Richter[3)], Toshihiro Tanaka[4)], Toshiaki Nakajima[5)], Sawa Kostin[3)]*, Toru Izumi[1)], Jutta Schaper[3)]* and Katsushi Tokunaga[2)]*

[1)]Department of Cardiovascular Medicine, Post-graduate School of Medicine, Kitasato University, [2)]Department of Human Genetics, Post-graduate School of Medicine, University of Tokyo, [3)]Department of Experimental Cardiology, Max-Planck Institute, Bad Nauheim, Germany, [4)]Laboratory for Cardiovascular Diseases, RIKEN, Yokohama, [5)] Department of Ischemic Circulatory Physiology, University of Tokyo, Japan.

*These authors equally contributed to the study.

A part of this report was presented as an introductory lecture of Albrecht Fleckenstein Award in the 17th International Congress of Heart Disease, Toronto, Canada, on July 29, 2012.

Present study was financially supported by the Research Grants from the Ministry of Education, Culture, Science and Sports, the Ministry of Health, Welfare and Labor, and the Motor Vehicle Foundation, Japan.

Correspondence to T. Toyo-oka, MD, PhD, Department of Cardiovascular Medicine, Post-graduate School of Medicine, Kitasato University, Japan. E-mail address to toyo3terry@gmail.com, fax address +81-3-3390-4322.

Preface

Heart failure (HF), a serious syndrome with diverse ethnicity and complicated etiology, is one of the leading causes of death. A part is heritable, though its underlying factors still remain elusive. GWAS (genome-wide association study) is promising for identifying the causative genes, directly or indirectly related genes as well as modifier genes that aggravate or ameliorate the clinical process to the advanced phase (1). This overview mainly focused our on-going HF-GWAS trial for the pathogenesis and/or progression of HF at the worldwide and whole genome levels, irrespective of the variable pathogenic factors common-in or specific-to different ethnicity, without missing biologically significant genes. We propose here a new concept of Bigenome (nuclear and mitochondrial)-Wide Association Study (BWAS) necessary for clarifying complexities of HF and providing therapeutic options.

Validity and Accuracy of a Case-Control Study

The case-control study has been defined as an observational epidemiological study of persons with the disease (or another outcome variable) of interest and "a suitable control group of persons without the disease (comparison group, reference group)". At a glance, it looks simple and persuasive but endogenously contains serious uncertainties. When in life-span? Under which circumstances and at where should be designated as the control group? What is "disease" or "normal"? Is it discernible to select candidate genes with majority rule? This paper aims not to discuss the medical determinism in case-control study but to realize an inevitable ambiguity to the principle of GWAS itself. The goal of GWAS targets identification of the potential, but often fuzzy gene(s), suggestive of a close or distant relationship to HF.

The current GWAS started as a post-genome project in Japan (Fig. 1). Genomic DNAs donated from the normal control and HF-cases and Affymetrix 6.0 for single nucleotide polymorphism (SNP)/single nucleotide variation (SNV)/ copy number variation (CNV) revealed ~1,500,000 haploid alterations and the

subsequent coding DNA sequence (CDS) analysis identified 7,287 SNPs with the χ^2 or Fisher's test. After restricting to the exons, or ORF, exon-intron border and stop codons, these SNPs reduced to ~1/3, consisting of 107 non-synonymous mutations, 54 stop codons, 23 insertion/deletions (in/del) to cause frame shift and 2,688 synonymous mutations (Fig. 2). These mutants did not overlap with Caucasian patients with dilated cardiomyopathy (1). Various cases with HF were diagnosed with clinical symptoms, physiological, morphological, biochemical and/or serological features. Candidate genes included adhesion molecules, channel proteins, cell signaling, transcription factors, proteases and anonymous proteins and would be opened elsewhere.

Evaluation of Candidate SNPs Related to Advanced HF

The SNP prevalence was analyzed with statistic test and the p value of each SNP was calculated with appropriate statistics. It should be notified that p values after Peason's χ^2 test or Fisher's exact test does not mean statistical potential of pathogenicity but denote the specificity. The Manhattan plot, –log (p) along the physical position on each chromosome, is critically dependent on case number. For the contribution potential to disease, effect size, β value, would be preferential. Both sex-chromosomes and mt-genes were excluded from this report, because they include many candidates to be commented and heteroplasmy, respectively, requiring other algorithms to discuss the genetic background (2-5).

Multiple Mutations in Each Nuclear Chromosome and Mitochondrion

The mutation locus was not disseminated but scattered in each autosome with some concentrated bias on 1, 2, 5, 11, 13, 15, 19 and 22 chromosomes (Fig. 3). These results may reflect natural selection under the *de novo* mutation and suggests the biological ontology, *i.e.* drastic modification of 2D/3D structure of the transcript or the transgene (4) may determine the viability or influence adoptability of mutants to environmental changes. These genetic modifications highlight the long-term mitochondrial (mt) symbiosis (5), because mt-genes often

show heteroplasmy or ethnicity-dependent haplogroup. More than 90% of nuclear SNPs are occupied by introns, pseudogenes or synonymous mutations (Fig. 3). In contrast, mt-gene has own exons, rRNAs and much less non-coding region in d-loop. Combination of nuclear and mt-SNPs are useful for identifying the haplogroup (3-5). Mt-mutations in heart require careful evaluation, since ORF-coding exons or tRNAs play a pivotal role in the ATP synthesis, reactive oxygen species (ROS) production, apoptosis induction and/or HF (3, 4).

A Novel Concept, "Bigenome-Wide Association Study (BWAS)", and Conclusion

In addition to nuclear genes, mt-gene also contributes to the incomparable pathophysiology at the cell/organ/body levels, particularly in muscular, cardiac and neural tissues (3) that require massive ATP. In addition to the nuclear gene, we intensify that mt-gene mutations should be considered along the time-course of HF and propose here a novel concept of BWAS, a combined research of nuclear and mt-genomes. This cross-talk between nuclear and mt-genes is different from the classic components located among mt-complexes coded by nuclear genes (NUMT, 3) and needed to maintain mt-function.

Our concept meant that combined mutations in nuclear and mt-gene may age-dependently aggravate HF and formed ROS synergistically peroxidizes adjacent constituents (DNAs, proteins or lipids), induce mutagenesis, reduce ATP production, enhance intracellular Ca^{2+} levels, decrease cardiac muscle cell contractility, activate endogenous proteases (1) and result in apoptosis and/or necrosis (1, 3, 6). Interruption of these sequential cascades would produce the beneficial outcome of the patients with HF. Compared with HF-related GWAS in European and African American (7), Japanese cases with HF indicated common SNPs to both ethnic groups. In addition, exome sequencing has recently revealed 25 % of causative loci in familial cases with exome-sequencing (8). Thus, we conclude that the gene analyses should be developed in both nuclear and mt-genomes and expanded to other candidate loci like iSNP, non-coding region (NCR) like miR to cover the whole aspects of genetic disorders.

References

1. Toyo-oka T, Kawada T, Nakata J, *et al.,* Translocation and cleavage of myocardial dystrophin as a common pathway to advanced heart failure: a scheme for the progression of cardiac dysfunction. *Proc Natl Acad Sci USA.* 101;7381-5, 2004.
2. Charchar FJ, Bloomer LD, Barnes TA, *et al.,* Inheritance of coronary artery disease in men: an analysis of the role of the Y chromosome. *Lancet* 379;915-22, 2012.
3. Wallace DC, Colloquium paper: bioenergetics, the origins of complexity, and the ascent of man. *Proc Natl Acad Sci USA* 107 (Suppl 2);8947-53, 2010.
4. Shin WS, Tanaka M, Suzuki J, *et al.,* A novel homoplasmic mutation in mtDNA with a single evolutionary origin as a risk factor for cardiomyopathy. *Am J Hum Genet.* 67;1617-20, 2000.
5. Toyo-oka T, Tanaka T, Toyo-oka L, *et al.,* In "*Genes and Cardiovascular Function*". Ostadal B. *et al.,* eds, Springer, pp85-92, 2011.
6. Toyo-oka T and Kumagai H. Cardiac troponin levels as a preferable biomarker of myocardial cell degradation. *Adv Exp Med Biol.* 592;241-9, 2007.
7. Smith NL, Felix JF, Morrison AC, *et al.,* Association of genome-wide variation with the risk of incident heart failure in adults of European and African ancestry: a prospective meta-analysis from the cohorts for heart and aging research in genomic epidemiology (CHARGE) consortium. *Circulation* (Cardiovasc Genet.) 3:256-66, 2010.

Figure Legends

Fig. 1. Road-map to identify pathogenic SNPs related to HF. All methods are informative, but still not definitive, because of gene interaction or cross-talk between candidate loci at each nt (epigenetic), intragenic (LD etc), intergenic (miR), and/or intergenomic (MUMT) complexities.

Fig. 2. Gene distribution of SNPs in exome or open-reading frame (ORF) of HF. Note that total SNP number is determined by the threshold of p value.

Fig. 3. Transgenomic distribution of SNP related with AdHF.multiple mutations in Accumulated Manhattan plots of >100 GWAS of HF-related SNP (B). Note that X-, Y-sex chromosomes and mt-gene contain the haplogroup linked to each algorithm (2, 5).

Fig. 4. Mutation numbers in each autosome indicating heterogeneous distribution of SNP.

Fig. 1

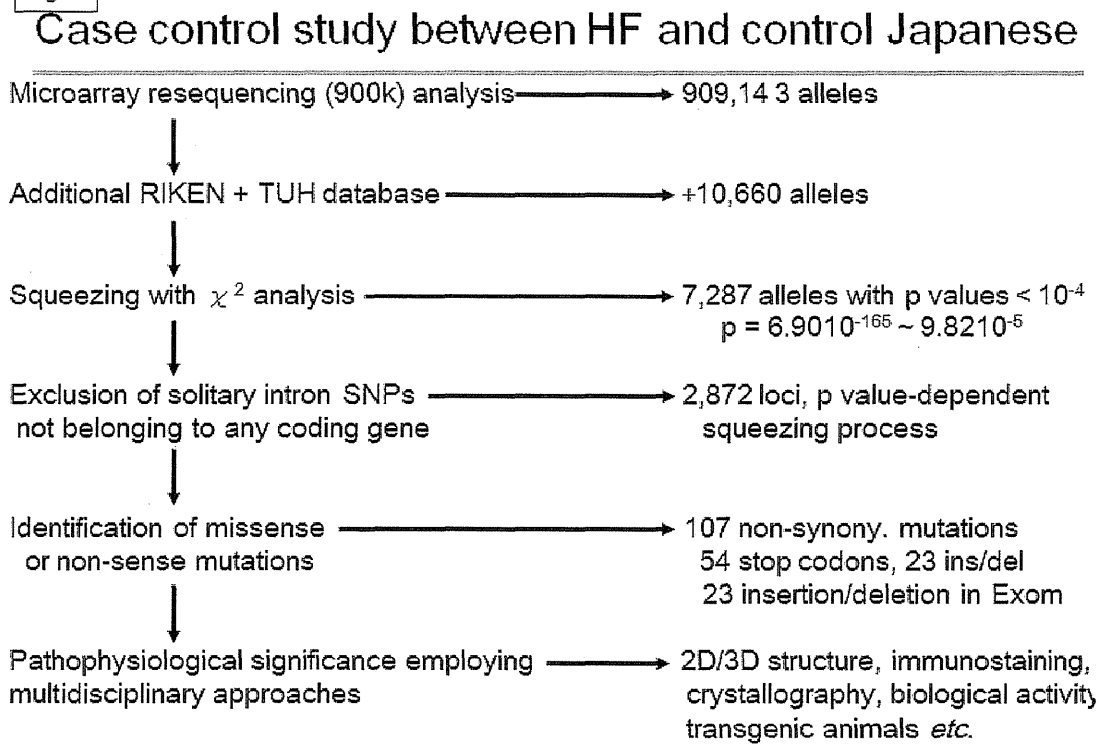
Case control study between HF and control Japanese
Microarray resequencing (900k) analysis
909,14 3 alleles
Additional RIKEN + TUH database
+10,660 alleles
Squeezing with χ^2 analysis
7,287 alleles with p values < 10^{-4}
p = 6.9010^{-165} ~ 9.8210^{-5}
Exclusion of solitary intron SNPs not belonging to any coding gene
2,872 loci, p value-dependent squeezing process
Identification of missense or non-sense mutations
107 non-synony. mutations
54 stop codons, 23 ins/del
23 insertion/deletion in Exom
Pathophysiological significance employing multidisciplinary approaches
2D/3D structure, immunostaining, crystallography, biological activity transgenic animals *etc.*

Fig. 2

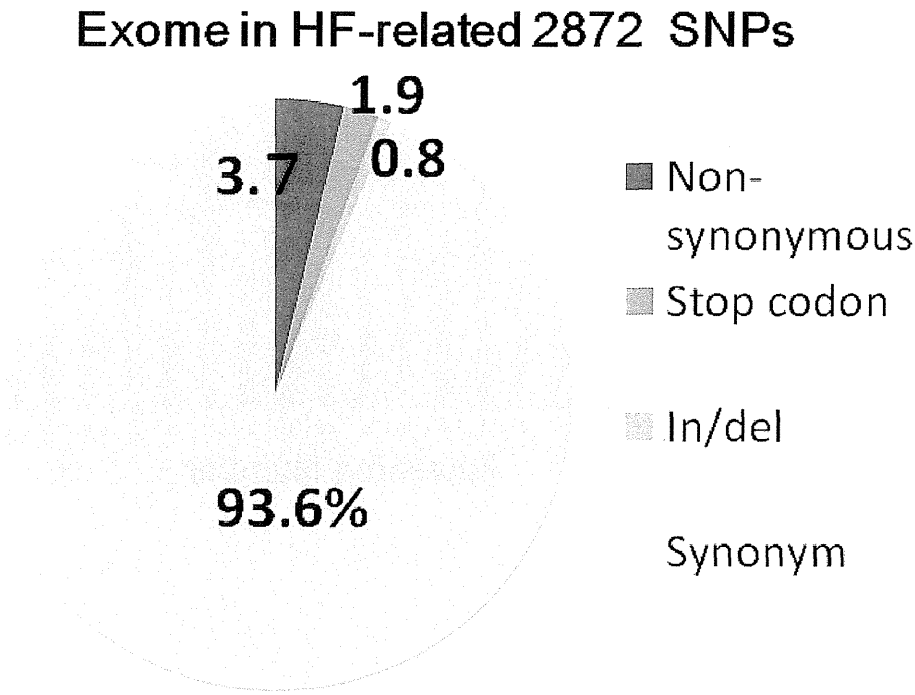
Exome in HF-related 2872 SNPs
1.9
0.8
3.7
93.6%
Non-synonymous
Stop codon
In/del
Synonym

Fig. 3

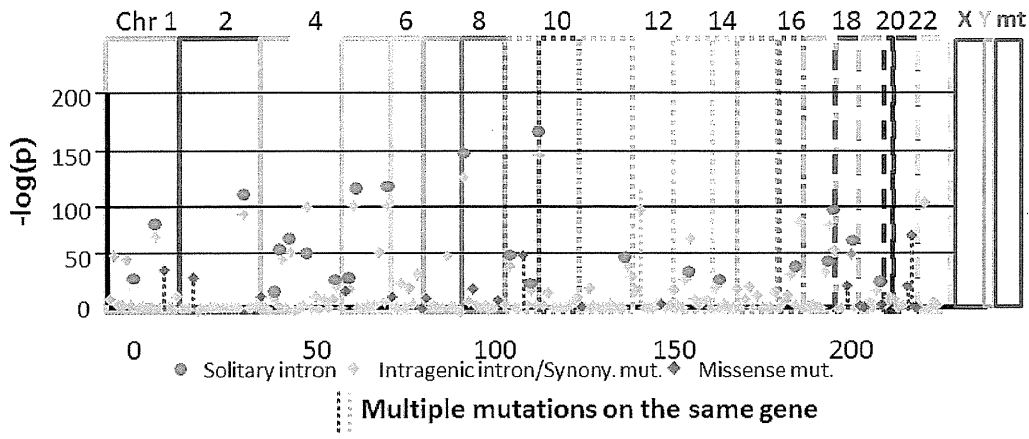
Chr 1 2 4 6 8 10 12 14 16 18 2022 X Y mt
200
150
100
50
0
-log(p)
0 50 100 150 200
Solitary intron
Intragenic intron/Synony. mut.
Missense mut.
Multiple mutations on the same gene

Fig. 4

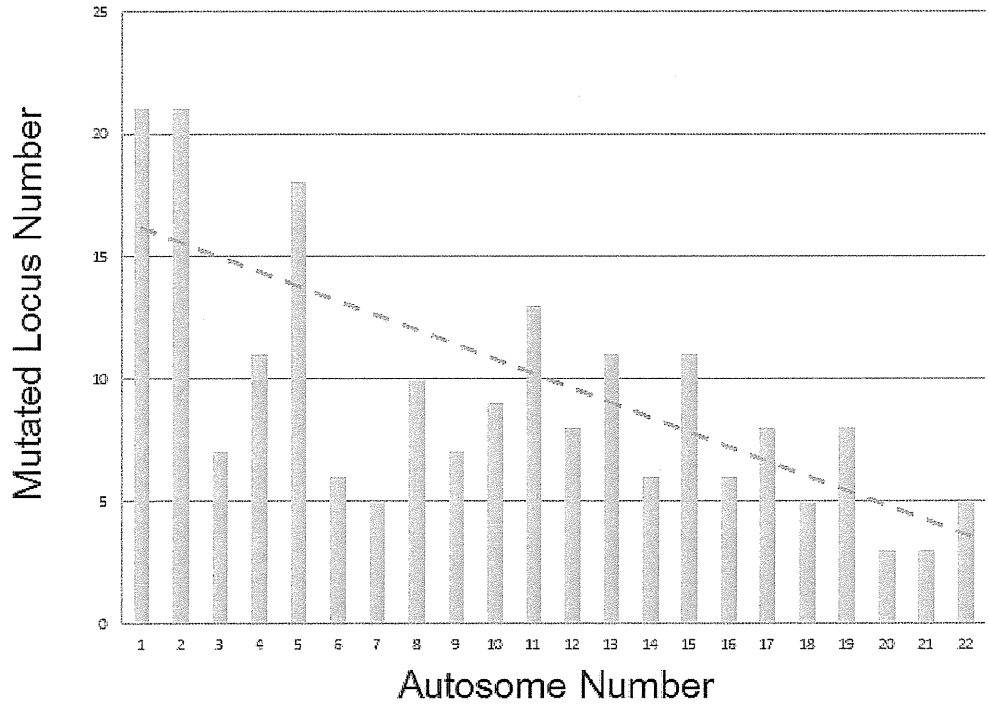
25
20
15
10
5
0
Mutated Locus Number
1 2 3 4 5 6 7 8 9 10 11 12 13 14 15 16 17 18 19 20 21 22
Autosome Number

Addendum

This monograph was planned to be published within 2012, but was delayed to Sep. 2013. During the interval, both case number and gene analyses proceeded and the authors add recent up-to-date SNP in March 2014 and displayed below. HF-related GWAS was reported in European American and African American (Smith *et al., Circulation, cardiovascular genet.,*3: 256-66, 2010) and some SNPs were coincided with our results in part (* ref. column in the table). Also, note that recent paper whole-exome sequencing (Yang *et al., N Engl J Med,* 369:1502-11; 2013) indicated 25% confirmation with in consecutive families with neurological diseases mainly.

E-mail address to TT was changed to toyo3terry@gmail.com.

Heart failure (HF)-related nuclear and mitochonsrial genome-wide association study (GWAS) in each chromosome and mitochondrion

chr. Number	gene number	approx. length (Mbp)	sequenced length	HF-realted allele #	HF/length (Mbp)	missense aa	nonsyn/ ORF	in/del, stop or ncRNA	total iSNP	total syn.	total CNV	ref.
1	>3000	240	~90%	45865	191	458	15.3%	228	39084	483	18213	*
2	>2500	240	~95%	56452	232	218	8.7%	175	40375	372	15969	*
3	1900	200	~95%	12579	64	30	1.6%	66	16773	59	3209	*
4	1600	190	~95%	26712	141	75	4.7%	49	11364	119	14375	
5	1700	180	> 95%	56291	313	193	11.4%	151	36541	304	4013	
6	1900	170	> 95%	48149	198	203	10.7%	218	13493	326	18213	
7	1800	150	> 95%	20389	136	97	5.4%	89	8989	181	11673	*
8	1400	140	> 95%	48527	347	28	2.0%	197	19211	0	13431	*
9	>1400	130	> 85%	41451	319	94	6.7%	148	3983	208	10653	*
10	>1400	130	> 95%	25083	193	70	5.0%	122	9960	65	6899	*
11	2000	130	> 95%	1480	11.0	12	0.6%	7	1141	20	379	*
12	1600	130	> 95%	42750	329	206	12.9%	159	17312	415	10170	*
13	800	110	> 80%	34063	310	76	9.5%	112	18242	138	9042	
14	1200	100	> 80%	27849	278	127	10.6%	116	14150	206	8341	
15	1200	100	> 80%	26121	261	122	10.2%	155	21526	261	6396	*
16	1300	90	> 85%	23237	258	46	3.5%	119	21166	251	7259	
17	1600	80	> 95%	9513	119	146	9.1%	105	8611	174	2295	
18	600	70	> 95%	11191	160	65	10.8%	31	6473	67	2636	
19	>1700	60	> 85%	7624	127	195	11.5%	106	5565	227	3391	*
20	900	60	> 90%	22807	360	179	19.9%	118	17587	217	6041	
21	400	40	> 70%	12537	313	57	14.3%	91	12340	88	3277	
22	800	40	~70%	11411	285	142	17.8%	121	10903	161	2925	
X	>1400	150	~95%	42323	282	220	15.7%	110	31142	313	9301	
Y	>366	50	~50%	366	7	0	0.0%	1	81	1	?	
mt	37	0.016569	complete	119	150602	25	150602.0%	2	0	63	5	
Umbiguous	116											
No assembly	44											
Sum	**~35000**	**2.93 Bbp**	**50~100%**	**~663800**		**3084**		**>2798**	**>385931**	**>4718**	**>188106**	

EUROPEAN SOCIETY OF CARDIOLOGY®

Cardiovascular Research (2013) 99. 461–470
doi:10.1093/cvr/cvt122

Deficiency of senescence marker protein 30 exacerbates angiotensin II-induced cardiac remodelling

Tomofumi Misaka[1], Satoshi Suzuki[1], Makiko Miyata[1], Atsushi Kobayashi[1], Tetsuro Shishido[2], Akihito Ishigami[3], Shu-ichi Saitoh[1], Masamichi Hirose[4], Isao Kubota[2], and Yasuchika Takeishi[1]*

[1]Department of Cardiology and Hematology, Fukushima Medical University, 1 Hikarigaoka, Fukushima 960-1295, Japan; [2]First Department of Internal Medicine, Yamagata University School of Medicine, Yamagata, Japan; [3]Molecular Regulation of Aging, Tokyo Metropolitan Institute of Gerontology, Tokyo, Japan; and [4]Department of Molecular and Cellular Pharmacology, Iwate Medical University School of Pharmaceutical Science, Iwate, Japan

Received 17 December 2012; revised 11 May 2013; accepted 15 May 2013; online publish-ahead-of-print 30 May 2013

Time for primary review: 37 days

Aims Ageing is an important risk factor of cardiovascular diseases including heart failure. Senescence marker protein 30 (SMP30), which was originally identified as an important ageing marker protein, is assumed to act as a novel anti-ageing factor in various organs. However, the role of SMP30 in the heart has not been previously explored. In this study, our aim was to elucidate the functional role of SMP30 on cardiac remodelling.

Methods and results SMP30 knockout (KO) mice and wild-type (WT) mice were subjected to continuous angiotensin II (Ang II) infusion. After 14 days, the extent of cardiac hypertrophy and myocardial fibrosis was significantly higher in SMP30-KO mice than in WT mice. Echocardiography revealed that SMP30-KO mice had more severely depressed systolic and diastolic function with left ventricular dilatation compared with WT mice. Generation of reactive oxygen species related with activation of nicotinamide adenine dinucleotide phosphate-oxidase was greater in SMP30-KO mice than in WT mice. The number of deoxynucleotidyl transferase-mediated dUTP nick end-labelling positive nuclei was markedly increased in SMP30-KO mice with activation of caspase-3, increases in the Bax to Bcl-2 ratio and phosphorylation of c-Jun N-terminal kinase compared with WT mice. Furthermore, the number of senescence-associated β-galactosidase-positive cells was significantly increased via up-regulation of p21 gene expression in SMP30-KO mice compared with WT mice.

Conclusion This study demonstrated the first evidence that deficiency of SMP30 exacerbates Ang II-induced cardiac hypertrophy, dysfunction, and remodelling, suggesting that SMP30 has a cardio-protective role in cardiac remodelling with anti-oxidative and anti-apoptotic effects in response to Ang II.

Keywords Senescence marker protein 30 (SMP30) • Ageing • Remodelling • Oxidative stress • Apoptosis

1. Introduction

The prevalence and mortality rate of heart failure dramatically increase in older people, and ageing is one of the risk factors for cardiovascular events.[1] With ageing, the heart shows changes in cardiac structure and function. Age-associated cardiac remodelling includes an enlargement of cardiomyocyte size, loss of myocytes due to apoptosis or necrosis, and increase of matrix connective tissue. These age-associated cardiac changes seem to be relevant to the steep increases in left ventricular hypertrophy, diastolic dysfunction, and subsequent heart failure.[2]

Oxidative stress is considered to be an important factor in controlling heart ageing.[3] It is well known that the renin–angiotensin system (RAS) is a central component of the physiological and pathological responses of the cardiovascular system. Activation of RAS is a significant driver of oxidative stress and is involved in age-related cardiac remodelling. Angiotensin II (Ang II), the primary effector molecule of RAS, contributes not only to vasoconstriction and hypertension, but also to cardiac hypertrophy, remodelling, and heart failure. Therefore, Ang II signalling appears to play a critical role in heart ageing.

* Corresponding author. Tel: +81 245471190; fax: +81 245481821. Email: takeishi@fmu.ac.jp

Senescence marker protein 30 (SMP30), a 34-kDa protein, was originally identified as a novel ageing marker protein in rat liver, whose expression decreases androgen-independently with age.[4] SMP30 transcripts are detected in almost all organs, and the SMP30 gene is highly conserved among numerous animal species including humans.[5] Intracellular localization of SMP30 is in the cytoplasm and perinuclear regions, and SMP30 exists in multiple forms under physiological conditions.[6] It has been demonstrated that SMP30 plays multifunctional roles as Ca^{2+} regulator (named as regucalcin),[7] anti-oxidant,[8] and enzymatic ability to hydrolyze di-isopropyl phosphorofluoridate.[9] Recently, SMP30 has been determined as gluconolactonase, which is involved in ascorbic acid (vitamin C) biosynthesis in mammals, whereas human beings are unable to synthesize vitamin C *in vivo* because of mutations in L-gulonolactone oxidase.[10]

SMP30-knockout (KO) mice have been generated[11] and showed a shorter life span than that of the wild-type (WT) mice on a vitamin C-deficient diet.[12] Using SMP30-KO mice, recent reports have demonstrated that SMP30 functions to protect cells from apoptosis in the liver[11] and that SMP30 has protective effects against age-associated oxidative stress in the brain[13] and lungs.[14] Furthermore, SMP30-KO mice have shown accelerated senescence in the kidney[15] and the worsening of glucose tolerance.[16] Taken together, SMP30 is assumed to behave as an anti-ageing factor. However, the role of SMP30 in the heart has not been previously explored.

We hypothesized that SMP30 has cardio-protective functions from harmful stimuli with anti-oxidative and anti-apoptotic effects. To test the hypothesis, we used SMP30-KO mice to examine the effects of SMP30 on Ang II-induced cardiac hypertrophy and remodelling *in vivo*.

2. Methods

For additional detailed methods, please see Supplementary material online..

2.1 Animal protocol

SMP30-KO (C57BL/6 background) mice were established as previously reported.[11] Drinking water containing vitamin C (1.5 g/L) was provided for the SMP30-KO mice to avoid vitamin C deficiency due to their inability to synthesize vitamin C *in vivo*.[10] After anaesthetizing the mice by i.p. injection of pentobarbital (50 mg/kg body weight), an osmotic minipump (ALZET micro-osmotic pump MODEL 1002, DURECT Co., Cupertino, CA, USA) was subcutaneously implanted, and Ang II (800 ng/kg/min) was continuously infused for 14 days.[17,18] Controls were administered saline. The investigations conformed to the *Guide for the Care and Use of Laboratory Animals* published by the US National Institutes of Health (NIH publication, 8th Edition, 2011). Our research protocol was approved by the institutional review board, and all animal experiments were conducted in accordance with the guidelines of Fukushima Medical University Animal Research Committee.

2.2 Measurement of vitamin C

Total vitamin C levels in the heart were measured by the dinitrophenylhydrazine method according to the manufacturer's protocol (SHIMA Laboratories Co. Ltd., Tokyo, Japan).[19]

2.3 Measurements of blood pressure and heart rate

Mice were implanted with a radiotelemetry probe (TA11PA-C22, Data Sciences International, St Paul, MN, USA) under i.p. anaesthesia by pentobarbital (50 mg/kg body weight) as described previously.[20] After a recovery phase of 10 days, basal arterial pressure and heart rate (HR) were started to recorded. After the measurement of control, Ang II was subcutaneously infused via an osmotic minipump, and the data were recorded.

2.4 Echocardiography

Transthoracic echocardiography was performed using Vevo 2100 High-Resolution *In Vivo* Imaging System (Visual Sonics, Inc., Toronto, Canada) with a high-resolution 40-MHz imaging transducer as previous reports described.[21,22] Mice were lightly anaesthetized by titrating isoflurane (0.5–1.5%) to achieve an HR of ~400 b.p.m., and all the measurements were obtained from three cardiac cycles.

2.5 Cardiac catheterization

The cardiac catheterization was performed as described previously.[23] Briefly, mice were anaesthetized by i.p. injection of 2,2,2-tribromo-ethanol (250 mg/kg body weight), the right carotid artery was cannulated with the micropressure transducer (samba preclin 420 LP, Samba Sensors AB, Gothenburg, Sweden) into the left ventricle. Adequacy of anaesthesia was monitored by HR, aortic blood pressure, and respiratory rate as well as the absence of reactions of painful stimuli. The data were measured using the Labscribe 2 software (iWorx Systems, Inc., Dover, NH, USA).

2.6 Histopathological analysis

After continuous infusion of Ang II or saline for 14 days, mice were sacrificed by cervical dislocation and hearts were rapidly excised. The paraffin-embedded heart sections were stained with haematoxylin and eosin or Elastica-Masson. The cross-sectional area of cardiomyocyte and fibrosis fraction was measured using the NIH ImageJ software (National Institutes of Health, Bethesda, MD, USA) and Adobe Photoshop CS2 (Adobe, San Jose, CA, USA).[24]

In immunohistochemical analysis, the paraffin-embedded sections were incubated with anti-SMP30 antibody (SHIMA Laboratories Co. Ltd., Tokyo, Japan) with a dilution of 1:200 or negative control (normal serum). The sections were stained with horseradish peroxidase-conjugated secondary antibody (Histofine Simple Stain Mouse MAX PO (R), Nichirei Biosciences, Inc., Tokyo, Japan) and diaminobenzidine etrahydrochloride, and counterstained with haematoxylin.

2.7 Assessment of reactive oxygen species generation

The fresh-frozen heart sections were incubated with 10 μmol/L dihydroethidium (DHE, Sigma-Aldrich Co., St Louis, MO, USA).[25,26] The fluorescent images were acquired using fluorescence microscope (Olympus IX71, OLYMPUS Optical Co., Tokyo, Japan) and the mean DHE fluorescence intensity of cardiomyocytes was quantitated with the NIH imageJ software.[26] In addition, 10 mmol/L apocynin, a nicotinamide adenine dinucleotide phosphate (NADPH) oxidase inhibitor, was provided in drinking water with Ang II continuous infusion, and reactive oxygen species (ROS) generation was evaluated by DHE staining.[27]

2.8 Western blotting

Total protein was extracted from the snap-frozen left ventricle using Cell Lysis Buffer (Cell Signaling Technology, Inc., Beverly, MA, USA) with Protease Inhibitor Cocktail (BD Biosciences, San Jose, CA, USA) as previous reports described.[24] The primary antibodies were as follows: anti-SMP30, anti-67^{phox}, anti-Bax, anti-Bcl-2, anti-phospho-stress-activated protein kinase/c-Jun N-terminal kinase (SAPK/JNK, Thr183/Tyr185), anti-SAPK/JNK (Cell Signaling Technology, Inc.), anti-activated-caspase-3 (Bioworld Technology, Inc., Minneapolis, MN, USA), and mouse anti-β-actin (Santa Cruz Biotechnology, Inc.). The signals from immunoreactive bands were visualized by an Amersham ECL system (Amersham Pharmacia Biotech UK Ltd., Buckinghamshire, UK) and quantified using densitometric analysis.

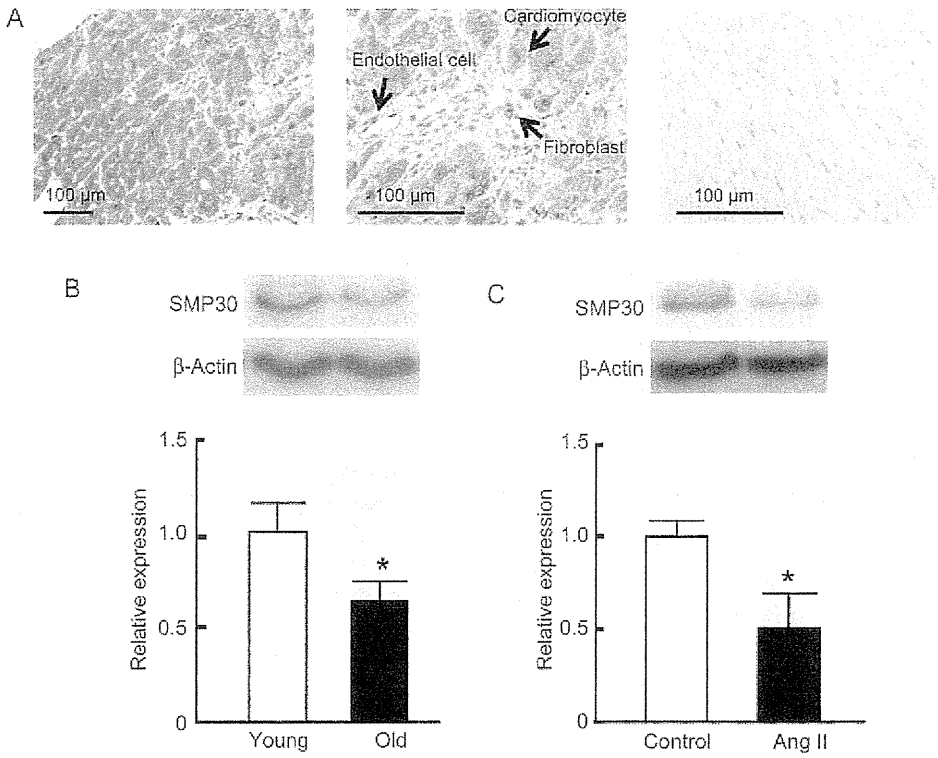

Figure 1 SMP30 expression in heart tissue. (*A*) SMP30 is expressed in cardiomyocytes, fibroblasts, and vascular endothelial cells (left, magnification ×200; middle, ×400). Right panel indicates negative control (×400). (*B*) Cardiac SMP30 expression was significantly decreased by 40% at 12-month-old WT mice (old) compared with 3-month-old WT mice (young). (*C*) Cardiac SMP30 expression was significantly decreased by 50% after Ang II infusion for 14 days in WT mice. Results are mean ± SD from 3 mice in each group. *$P < 0.05$ vs. young mice or control.

2.9 *In vivo* terminal deoxynucleotidyl transferase-mediated dUTP nick end- labellingassay

Apoptosis was detected by the terminal deoxynucleotidyl transferase-mediated dUTP nick end-labelling (TUNEL) method (CardioTACS *In Situ* Apoptosis Detection Kit, Trevigen, Inc., Gaithersburg, MD, USA) according to the manufacturer's instructions. TUNEL-positive nuclei were counted, and then expressed as a per cent of the total nuclei.[28]

2.10 Senescence-associated β-galactosidase activity

Senescence-associated β-galactosidase (SA-β-gal) staining was performed according to the manufacturer's protocol (BioVision, Inc., Mountain View, CA, USA).[29] SA-β-gal-positive cardiomyocytes were visualized as blue colour under light microscopy, and positive cells for SA-β-gal activity were counted.

2.11 Reverse transcription polymerase chain reaction

Total RNA was extracted from the snap-frozen left ventricle using TRIzol reagent (Invitrogen, Carlsbad, CA, USA).[28] Reverse transcription polymerase chain reaction (RT–PCR) was performed using the PrimeScript RT–PCR Kit (Takara Bio, Inc., Otsu, Japan) according to the manufacturer's instructions. Primers were designed on the basis of GenBank sequences (p21, NM_001111099 and β-actin, NM_007393). The optical density of the bands was quantified using the NIH imageJ software.

2.12 Statistical analysis

All data were expressed as mean ± SD. Comparisons of vitamin C levels at basal conditions between WT mice and SMP30-KO mice were performed by an unpaired *t*-test. All other parameters were evaluated by two-way analysis of variance followed by multiple comparisons with the Bonferroni test using SPSS Statistics 17.0 (SPSS Japan, Inc., Tokyo, Japan). A probability value < 0.05 was considered statistically significant.

3. Results

3.1 Vitamin C levels of the heart tissue in WT mice and SMP30-KO mice

First, we measured vitamin C levels of the heart tissue in basal conditions. To avoid vitamin C deficiency, drinking water containing sufficient vitamin C was supplied for SMP30-KO mice because SMP30-KO mice were unable to synthesize vitamin C due to the lack of gluconolactonase.[10] The tissue concentrations of the vitamin C level were not significantly different between WT mice and SMP30-KO mice (45.7 ± 7.0 vs. 44.5 ± 10.2 μg/g tissue).

3.2 SMP30 expression in the heart tissue

Immunostaining revealed that SMP30 was expressed in cardiomyocytes, fibroblasts, and vascular endothelial cells in WT mice on the basis of cellular morphological characteristics (*Figure 1A*).[30] We confirmed the decrease in SMP30 expression with ageing in the WT mouse heart as

Table 1 Gravimetric and hemodynamic data of WT and SMP30-KO mice

	Control		Ang II	
	WT	SMP30-KO	WT	SMP30-KO
Gravimetric data				
BW, g	26.7 ± 1.1	27.8 ± 1.6	25.6 ± 1.5	27.2 ± 2.2
HW/TL, mg/mm	6.1 ± 0.6	6.5 ± 0.5	7.5 ± 0.6**	8.4 ± 1.0**†
LVW/TL, mg/mm	4.2 ± 0.5	4.6 ± 0.3	5.7 ± 0.5**	6.7 ± 0.9**††
Telemetry blood pressure				
HR, b.p.m.	612 ± 48	627 ± 50	593 ± 24	607 ± 65
SBP, mmHg	115.5 ± 12.4	114.8 ± 10.8	140.8 ± 8.6**	144.1 ± 13.7**
DBP, mmHg	85.1 ± 9.4	89.9 ± 9.6	129.4 ± 7.0**	128.6 ± 10.6**
MAP, mmHg	97.8 ± 11.6	99.9 ± 10.4	119.0 ± 6.2**	115.2 ± 9.7**
Echocardiography				
LVEDD, mm	3.77 ± 0.37	3.77 ± 0.38	3.68 ± 0.31	4.26 ± 0.21**††
LVESD, mm	2.52 ± 0.32	2.42 ± 0.42	2.52 ± 0.35	3.12 ± 0.33**††
FS, %	33.2 ± 4.4	33.7 ± 4.1	31.8 ± 4.7	25.9 ± 5.2**††
Catheterization				
LVEDP, mmHg	5.2 ± 1.6	6.0 ± 1.7	9.8 ± 1.0*	11.7 ± 3.0**
max dP/dt, mmHg/s	11 556 ± 850	10 977 ± 940	11 675 ± 999	7303 ± 1107**††
min dP/dt, mmHg/s	8140 ± 668	8247 ± 384	7582 ± 1408	4804 ± 1897*†
Tau, ms	4.8 ± 2.0	4.3 ± 0.3	6.3 ± 1.9**	8.3 ± 1.9**

Data are presented as mean ± SD from 10 to 15 mice in each group.
BW, body weight; HW, heart weight; LVW, left ventricular weight; TL, tibial length; HR, heart rate; SBP, systolic blood pressure; DBP, diastolic blood pressure; MAP, mean arterial pressure; LVEDD, left ventricular end-diastolic dimension; LVESD, left ventricular end-systolic dimension; FS, fractional shortening; LVEDP, left ventricular end-diastolic pressure; max and min dP/dt, maximal and minimal rates of left ventricular pressure development, respectively; Tau, time constant of left ventricular isovolumic relaxation.
*$P < 0.05$ and **$P < 0.01$ vs. control in the same strain mice; †$P < 0.05$ and ††$P < 0.01$ vs. Ang II-infused WT mice.

described previously in other organs.[4] Cardiac SMP30 was significantly decreased by 40% at 12-month-old WT mice compared with 3-month-old WT mice ($P < 0.05$, *Figure 1B*). Additionally, cardiac expression of SMP30 was significantly decreased by 50% after Ang II infusion for 14 days in 3-month-old WT mice, suggesting that the expression of SMP30 may alter in cardiovascular diseases ($P < 0.05$, *Figure 1C*).

3.3 Effect of SMP30 deficiency on Ang II-induced cardiac hypertrophy and fibrosis

As shown in *Table 1*, heart weight (HW) and left ventricular weight (LVW) corrected by the tibial length (TL) were similar between control WT mice and SMP30-KO mice. After Ang II infusion, the ratios of HW to TL and LVW to TL were significantly higher in SMP30-KO mice than in WT mice ($P < 0.05$ and $P < 0.01$, respectively), although the blood pressure was similarly elevated in both Ang II-infused WT mice and SMP30-KO mice by telemetry blood pressure monitoring (*Table 1*).

Histological examination showed that Ang II-infused SMP30-KO mice had substantial left ventricular hypertrophy with left ventricular dilatation compared with Ang II-infused WT mice, which suggested eccentric hypertrophy in Ang II-infused SMP30-KO mice compared with concentric hypertrophy in Ang II-infused WT mice (*Figure 2A*, top). The cardiomyocyte cross-sectional area was significantly larger in Ang II-infused SMP30-KO mice than in Ang II-infused WT mice (399 ± 17 vs. 372 ± 11 μm^2, $P < 0.01$, *Figure 2A*, middle and *B*). Additionally, *ex vivo* analysis demonstrated that cell width, length, and surface area of isolated cardiomyocytes were significantly greater in SMP30-KO mice than in WT mice after Ang II stimulation (Supplementary material online, *Figure S1*). The degree of cardiac fibrosis was significantly higher in Ang II-infused SMP30-KO mice than in Ang II-infused WT mice (6.4 ± 0.8 vs. 7.5 ± 0.7%, $P < 0.01$, *Figure 2A*, bottom and *C*). These data revealed that the deficiency of SMP30 exacerbates Ang II-induced cardiac hypertrophy and fibrosis, independently of blood pressure.

3.4 Effect of SMP30 deficiency on Ang II-induced cardiac dysfunction

As shown in *Table 1*, there were no differences in cardiac function between WT mice and SMP30-KO mice under basal conditions. Echocardiography showed that left ventricular end-diastolic and end-systolic dimensions were enlarged and fractional shortening was reduced in SMP30-KO mice compared with WT mice at 14 days after Ang II infusion ($P < 0.01$, *Table 1* and Supplementary material online, *Table S1* and *Figure S2*, top). The left ventricular mass was greater in Ang II-infused SMP30-KO mice than in Ang II-infused WT mice, which was concordant with the histological findings ($P < 0.01$). Ang II-infused SMP30-KO mice had significantly higher peak E velocity, *E/A*, and *E/E'* compared with Ang II-infused WT mice (Supplementary material online, *Table S1* and *Figure S2*, middle and bottom). The mitral inflow showed the restrictive pattern in Ang II-infused SMP30-KO mice in contrast to the relaxation abnormality pattern or the pseudo-normalization pattern in Ang II-infused WT mice. These echocardiographic data revealed that left ventricular systolic and diastolic functions were remarkably depressed in SMP30-KO mice compared with WT mice after Ang II infusion.

Haemodynamic assessment by cardiac catheterization showed that max dP/dt and min dP/dt were significantly lower in SMP30-KO mice than in WT mice after Ang II infusion ($P < 0.01$ and $P < 0.05$,

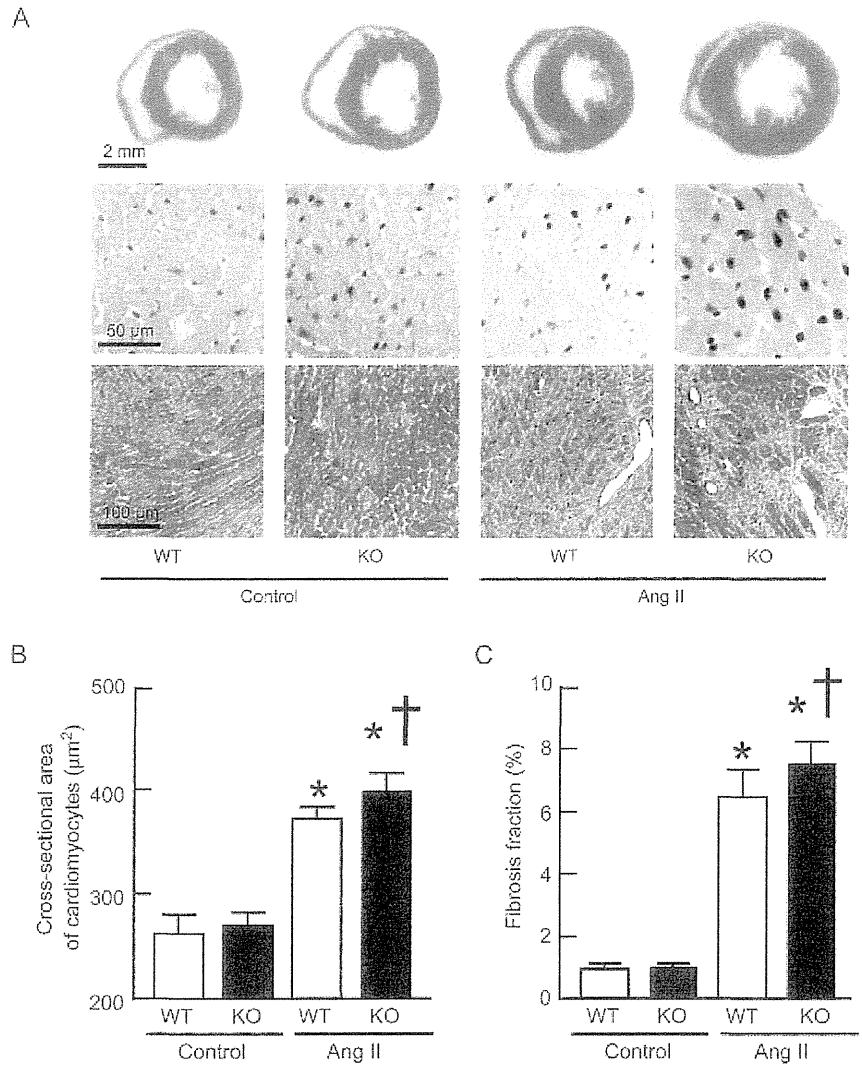

Figure 2 Cardiac hypertrophy and fibrosis in WT and SMP30-KO mice after Ang II infusion. (*A*) Representative images of light micrographs of hearts from WT and SMP30-KO mice with and without Ang II infusion (top). Haematoxylin and eosin staining of myocardial cross-sections (middle). Elastica-Masson staining of myocardial sections (bottom). (*B*) Quantitative analysis of the cross-sectional area of cardiomyocytes from the left ventricle. (*C*) The per cent area of myocardial interstitial fibrosis in the left ventricle. Data are presented as mean ± SD from 6 to 8 mice in each group. *$P < 0.01$ vs. control in the same strain mice; †$P < 0.01$ vs. Ang II-infused WT mice.

respectively), supporting that cardiac systolic and diastolic functions were more severely depressed in SMP30-KO mice (*Table 1*).

3.5 Effect of SMP30 deficiency on Ang II-induced myocardial oxidative stress

We examined myocardial oxidative stress by DHE staining which indicates the O_2levels of living cells because oxidative stress is considered to be one of the important mechanisms of heart failure and cardiac remodelling. Although Ang II infusion dramatically increased the ROS generation in both WT mice and SMP30-KO mice, the ROS generation in Ang II-infused SMP30-KO mice was significantly greater than in Ang II-infused WT mice ($P < 0.01$, *Figure 3A*). In addition, we found that the level of superoxide generation was significantly decreased in Ang II-infused WT mice with apocynin treatment, compared with that of Ang II-infused WT mice without apocynin treatment ($P < 0.01$, *Figure 3A*). As well as WT mice, SMP30-KO mice revealed that Ang II-induced superoxide generation was significantly down-regulated by apocynin treatment ($P < 0.01$, *Figure 3A*).

To investigate the involvement of NADPH oxidase in Ang II-induced ROS generation, we examined the expression of $p67^{phox}$ subunit of NADPH oxidase by western blotting. The expression levels of $p67^{phox}$ were significantly elevated in Ang II-infused SMP30-KO mice compared with Ang II-infused WT mice ($P < 0.01$, *Figure 3B*). These data suggested that the deficiency of SMP30 increased Ang II-induced myocardial oxidative stress via up-regulation of NADPH oxidase.

3.6 Effect of SMP30 deficiency on Ang II-induced apoptosis

As previously demonstrated, SMP30 has anti-apoptotic effects in other organs.[11] We, therefore, checked apoptosis using TUNEL staining

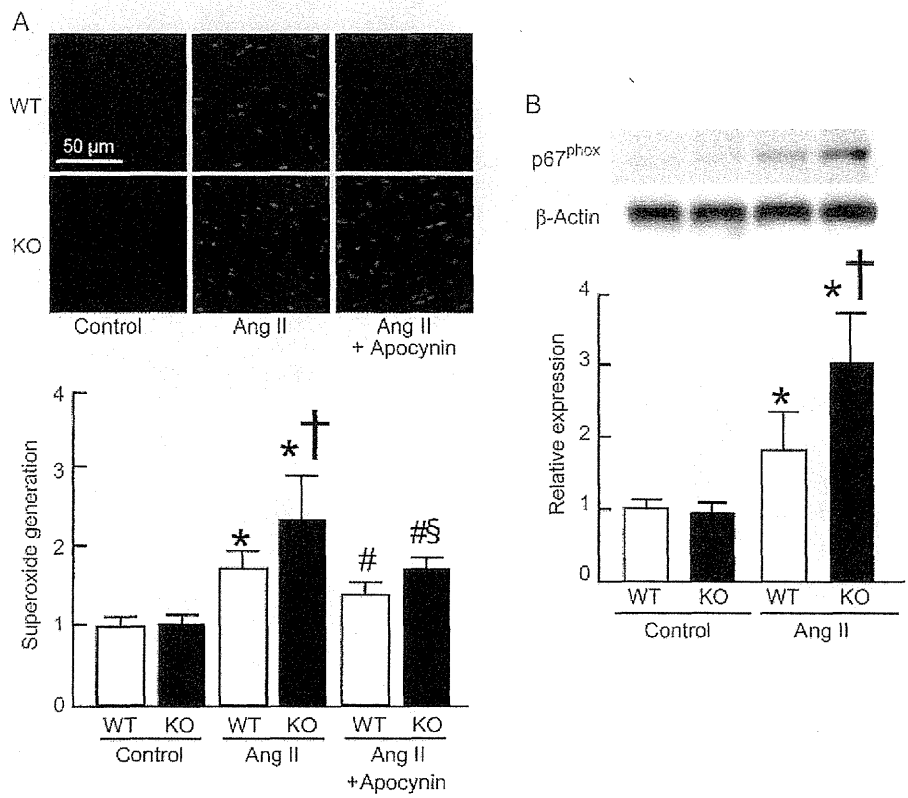

Figure 3 Myocardial oxidative stress in WT and SMP30-KO mice after Ang II infusion. (*A*) Upper panels show representative DHE staining of frozen left ventricular tissues. Lower bar graphs show quantification of superoxide generation. (*B*) Expression of $p67^{phox}$ of NADPH oxidase subunits was analysed by western blotting. Expression levels were expressed relative to those of β-actin. Results are mean ± SD from 6 to 10 mice in each group. $^{*}P < 0.01$ vs. control in the same strain mice; $^{\dagger}P < 0.01$ vs. Ang II-infused WT mice. $^{\#}P < 0.05$ vs. Ang II-infused mice in the same strain; $^{\S}P < 0.05$ vs. Ang II-infused WT mice with apocynin treatment.

(*Figure 4A*). After Ang II infusion, the numbers of TUNEL-positive nuclei including cardiomyocytes and non-cardyomyocytes were increased in both WT and SMP30-KO mice. The numbers of TUNEL-positive nuclei in Ang II-infused SMP30-KO mice were remarkably greater than in Ang II-infused WT mice, as shown in *Figure 4A* ($P < 0.01$).

Then, we examined signalling pathways of Ang II-induced apoptosis in the heart. Caspase-3 is a key mediator of apoptosis, and activation of caspase-3 leads to DNA injury and subsequently apoptotic cell death.[31] The activation of caspase-3 was induced by Ang II infusion in both WT and SMP30-KO mice, and the activation of caspase-3 in Ang II-infused SMP30-KO mice was significantly greater than in Ang II-infused WT mice ($P < 0.01$, *Figure 4B*). After Ang II infusion, Bax expression which functions as pro-apoptotic protein was increased, whereas the expression of anti-apoptotic protein Bcl-2 was decreased in both genotypes of mice. The ratio of Bax to Bcl-2 was significantly higher in Ang II-infused SMP30-KO mice than in Ang II-infused WT mice ($P < 0.01$, *Figure 4C*). Furthermore, we examined the involvement of SAPK/JNK which has a crucial role in cell apoptosis as one main subgroup of the mitogen-activated protein kinase family.[32] Phosphorylation activity of SAPK/JNK in Ang II-infused SMP30-KO mice was significantly increased compared with Ang II-infused WT mice ($P < 0.01$, *Figure 4D*). These findings demonstrated that SMP30 deficiency exacerbates Ang II-induced apoptosis through these signalling pathways.

3.7 Expression of senescence markers in SMP30-KO mice after Ang II infusion

Senescent cells can be identified by the expression of enzymatic SA-β-gal activity in left ventricular tissues (*Figure 5A*). SA β-gal activity was induced by Ang II stimulation. The numbers of SA β-gal-positive cells were significantly greater in Ang II-infused SMP30-KO mice than in Ang II-infused WT mice (1.7 ± 0.8 vs. $0.6 \pm 0.5/mm^3$, $P < 0.01$) as demonstrated in *Figure 5A*.

To evaluate the gene expression of cell cycle inhibitor to confirm senescence of cardiomyocytes, we analysed mRNA expression of p21 gene by RT–PCR (*Figure 5B*). Following Ang II infusion, the expression levels of p21 mRNA were increased in both WT mice and SMP30-KO mice. Compared with Ang II-infused WT mice, Ang II-infused SMP30-KO mice showed a significant increase in p21 expression ($P < 0.01$). These results indicate that deficiency of SMP30 induced cellular senescence after Ang II infusion by the p21-dependent pathway.

4. Discussion

Previous studies have shown that SMP30 acts as an anti-ageing factor, and SMP30 prevents oxidative stress and apoptosis in the liver, lungs, and brain.[11,13,14] However, the role of SMP30 in the heart has not